



21 YEARS OF BALKAN
TRIBOLOGICAL ASSOCIATION



ROMANIAN TRIBOLOGY
ASSOCIATION



UNIVERSITY PETROLEUM-GAS OF
PLOIESTI, ROMANIA

BALKANTRIB'14

8th INTERNATIONAL CONFERENCE ON TRIBOLOGY, 30th Oct.-1st Nov. 2014, SINAIA, ROMANIA

Theoretical and experimental analysis of friction forces acting on a flywheel energy storage system rotating in air

Victor Gabriel Marian^{1)*}, Tiberiu Laurian¹⁾, Radu Florin Mirică¹⁾, Adrian Pascu¹⁾, Petre Lucian Seiciu¹⁾

¹⁾ Department of Machine Elements and Tribology, University "Politehnica" Bucharest, Romania

*Corresponding author: victormarian@omtr.pub.ro

Complete address to which correspondence should be sent:

Conf.dr.ing. Victor Gabriel MARIAN, Department of Machine Elements and Tribology, Faculty on Mechanical Engineering and Mechatronics, University Politehnica of Bucharest, spl. Independenței 313, 060042 Bucharest, Romania

Abstract: Due to the high fuel price and environmental issues, reducing fuel consumption in the transportation sector became a major priority for both industry and research. One way of solving these problems is using a high speed flywheel for the energy storage. In order to minimize friction loss, the flywheel can be situated in a vacuum atmosphere. However, this can induce high costs. A cheaper solution is helium. The present paper aims to determine experimentally the friction losses of a flywheel rotating in air and compare the obtained results with theoretical models found in literature. The presented results can be extrapolated for helium as surrounding gas.

Keywords: friction, flywheel, energy storage, rotating cylinder, ecological transportation

1. Notations

b – flywheel height

c_M – drag coefficient of the upper and lower surface

c_{mc} – drag coefficient for the outer rim

ρ_{air} – air density

ω – angular velocity of the flywheel

d – flywheel diameter

h – flywheel height

$Re = \frac{\omega d^2}{4\nu}$ – Reynolds number

M_{fbb} – frictional torque of the deep groove ball bearings

M_{rr} – rolling frictional moment of the deep groove ball bearings

M_{sl} – sliding frictional moment of the deep groove ball bearings

M_{seal} – frictional moment of the seals of the deep groove ball bearings

M_{drag} – frictional moment of drag losses, churning, splashing etc. of the deep groove ball bearings

M_{fdisk} – friction torque on the upper and lower surface

M_{frim} – friction torque on the outer rim

M_{fair} – total air friction torque

ν – kinematic viscosity of air

2. Introduction

Due to the high fuel price and environmental issues, reducing fuel consumption in the transportation sector became a major priority for both industry and research. One way of solving these problems is using a high speed flywheel for the energy storage. The first flywheel powered bus was put into circulation in 1953 in Yverdon (Switzerland) [1]. It was produced by the company Oerlikon. The bus could travel without charging around 6 kilometers [2], but there were charging stations each 4 kilometers along the road.

Another method of reducing pollution consists in recovering the kinetic energy of the vehicle during the braking process [3].

The rotor of the flywheel can be manufactured using composite materials, thus obtaining a higher energy per kilogram of material [4]-[9]. The second advantage of composite materials is that they gradually disintegrate. Along magnetic bearings [10]-[11], hydrodynamic bearings were also used to support the flywheel.

In order to overcome the air friction, the flywheel is rotating in vacuum or helium environment.

However, vacuum systems are expensive, so a deep analysis should be made in order to evaluate the air friction loss. The results can also be extrapolated in order to evaluate the friction losses in a helium environment. The present article aims to determine experimentally the friction loss of a flywheel rotating in air and compare the obtained results with theoretical models found in the literature.

3. Experimental setup

The test rig is presented in Figure 1 and Figure 2. The flywheel (4) is made of steel, having an external diameter

Victor Gabriel MARIAN, Tiberiu LAURIAN, Radu Florin MIRICĂ, Adrian PASCU, Petre Lucian SEICIU of 243 mm and a width of 28 mm. The flywheel is supported by two deep groove ball bearings (3) in radial direction. The deep groove ball bearings are self-lubricated and have an internal diameter of 10 mm and an external diameter of 26 mm. The flywheel is also axially supported by a permanent magnetic axial bearing (5). The axial bearing consists of neodymium permanent ring magnets having an inner diameter of 16 mm and an outer diameter of 26 mm, providing sufficient repelling force in order to sustain the flywheel. The rotational speed of the flywheel is measured by an infrared light speed sensor (1) and a data acquisition device (2) connected to a computer.

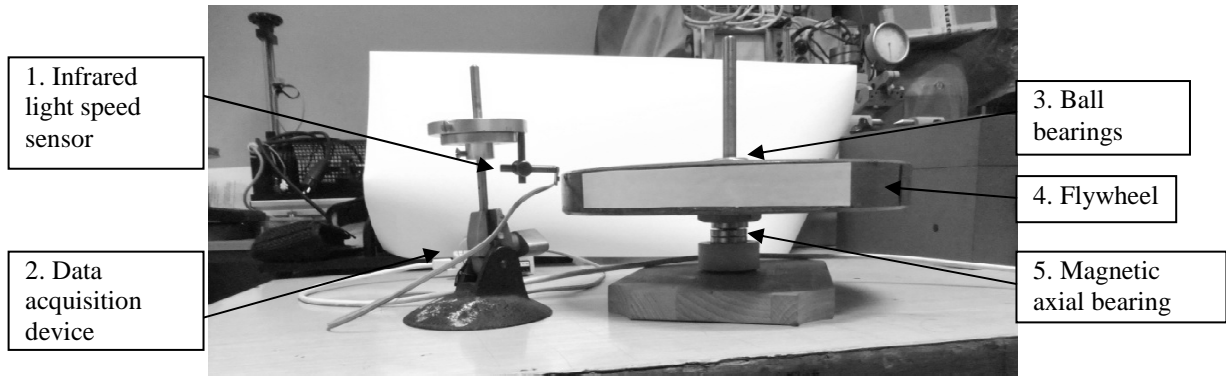


Figure 1 *Experimental arrangement for rotation speed measurement*

In order to measure the radial force that acts on the ball bearings, the flywheel system was fixed on an air bearing slider (2). Compressed air is supplied by the compressor (4). The centrifugal force was measured by a force sensor (3) which direction corresponds to that of the linear air bearing slider. The force sensor is a strain gauge based force sensor. The resistance variation of the strain gauge was measured by a National Instruments data acquisition system which has an incorporated strain bridge.



Figure 2 *Experimental arrangement for the measurement of centrifugal force*

4. Theoretical model

Two types of models were used for the theoretical analysis: analytical models and a numerical model using computational fluid dynamics software. A draft of the flywheel is presented in Figure 3 .

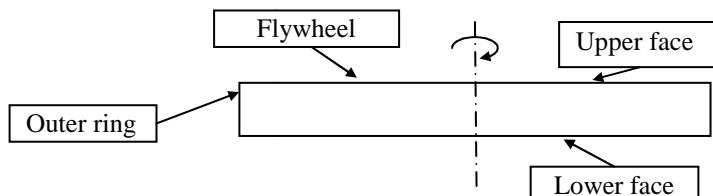


Figure 3 *Schematic of the flywheel*

4.1. Analytical model

4.1.1 Friction torque on the frontal faces of the flywheel

The friction torque on the upper and lower walls can be computed using the following formula [13], developed for a thin disk:

$$M_{f,disk,1} = \frac{c_M \rho \omega^2}{2} \left(\frac{d}{2} \right)^5 \quad (1)$$

where the drag coefficient c_M is considered to be

$$c_M = \begin{cases} \frac{5.2}{\sqrt{\text{Re}}} & \text{if } \text{Re} < 5 \cdot 10^5 \\ 0.168 & \text{if } \text{Re} > 5 \cdot 10^5 \\ \frac{0.168}{\sqrt[3]{\text{Re}}} & \end{cases} \quad (2)$$

A similar expression was used in [17] that cite [18]:

$$M_{f,disk,2} = c_W \cdot \pi \cdot \rho \cdot \omega^2 \cdot \left(\frac{d}{2} \right)^5, \quad (3)$$

where the drag coefficient c_W is:

$$c_W = \begin{cases} 3.87 \cdot \frac{1}{2\pi} \cdot \text{Re}^{-\frac{1}{2}} & \text{if } \text{Re} < 3 \cdot 10^5 \\ 0.1463 \cdot \frac{1}{2\pi} \cdot \text{Re}^{-\frac{1}{5}} & \text{if } \text{Re} > 3 \cdot 10^5 \end{cases} \quad (4)$$

When dividing $M_{f,disk,1}$ to $M_{f,disk,2}$ in the case of laminar flow we obtain 0.71.

Neue Hütte [19] proposes the same expression (1) to calculate the friction torque on frontal faces of a disc but the drag coefficient differs:

$$c_M = \begin{cases} \frac{64}{3} \cdot \frac{1}{\text{Re}} & \text{if } \text{Re} < 30 \\ \frac{3.84}{\sqrt{\text{Re}}} & \text{if } 30 < \text{Re} < 3 \cdot 10^5 \\ \frac{0.146}{\sqrt[5]{\text{Re}}} & \text{if } \text{Re} > 3 \cdot 10^5 \end{cases} \quad (5)$$

The expression used in [15] (following [16]) developed for flywheels contains inexplicitly the drag coefficient:

$$M_{f,disc} = 0.0364 \cdot v^{0.2} \cdot \rho \cdot \left(\frac{d}{2} \right)^{4.6} \cdot \omega^{1.8}. \quad (6)$$

with v in $[mm^2/s]$.

The expression can be rewrite into the form:

$$M_{f,disc} = 0.0364 \cdot \frac{v^{0.2}}{(d/2)^{2 \cdot 0.2} \cdot \omega^{0.2}} \cdot \rho \cdot \left(\frac{d}{2} \right)^5 \cdot \omega^2 = \frac{0.0728}{\text{Re}^{0.2}} \cdot \frac{1}{2} \cdot \rho \cdot \left(\frac{d}{2} \right)^5 \cdot \omega^2 = c_M \cdot \frac{1}{2} \cdot \rho \cdot \left(\frac{d}{2} \right)^5 \cdot \omega^2 \quad (7)$$

$$\text{with } c_M = \frac{0.0728}{\text{Re}^{0.2}}. \quad (8)$$

Practically the expression (1) is maintained but the drag coefficient is different. It is to remark that the presented methods differ only by the drag coefficient.

The results are presented in Figure 4 . We can remark that only the results presented in [15] and [16] are significantly higher compared to the others. The curve called ETH Zürich is coincident with the values presented in Neue Hutte.

4.1.2 Friction torque on the outer ring

The friction torque on the outer ring is considered to be [14]:

$$M_{frim} = 0.5 \cdot \pi \cdot \rho_{air} \cdot \omega^2 \left(\frac{d}{2} \right)^4 \cdot b \cdot c_{mc} \quad (9)$$

where the drag coefficient is considered to be

$$c_{mc} = \begin{cases} \frac{8}{Re} & \text{if } Re < 60 \\ \text{results from: } \frac{1}{\sqrt{c_{mc}}} = -0.8572 + 1.25 \cdot \ln(Re \cdot \sqrt{c_{mc}}) & \text{if } Re > 60 \end{cases} \quad (10)$$

A similar expression was used in [17] that cites [18]:

$$M_{f,rim} = c_w \cdot \pi \cdot \rho \cdot \omega^2 \cdot \left(\frac{d}{2}\right)^4 \cdot b. \quad (11)$$

$$c_w = \begin{cases} \frac{8}{Re} & \text{if } Re < 170 \\ \text{results from: } \frac{1}{\sqrt{c_w}} = -0.6 + 4.071 \cdot \log(Re \cdot \sqrt{c_w}) & \text{if } Re > 170 \end{cases} \quad (12)$$

Another expression is presented in [15] that cites [16]:

$$M_{f,rim} = 0.0298 \cdot v^{0.2} \cdot \rho \cdot b \cdot d^{-0.3} \cdot \left(\frac{d}{2}\right)^{3.9} \cdot \omega^{1.8} \quad (13)$$

with v in $[mm^2/s]$.

The results are presented in Figure 4 .

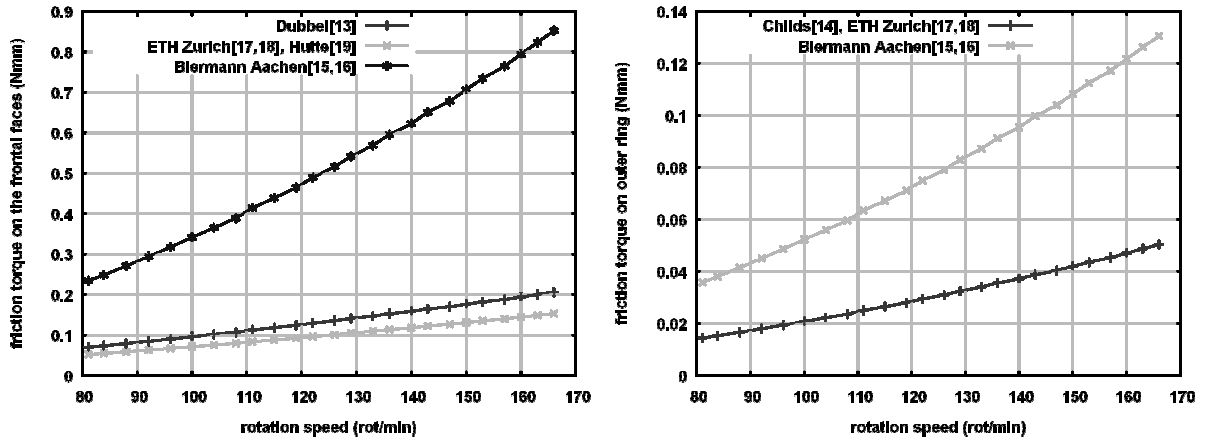


Figure 4 Analytical friction torque on the frontal faces and outer ring function of rotation speed

The values of the friction torque presented in [17] and [18] are extremely close to the values presented in [14].

4.1.3 Total analytical friction torque of the flywheel with air

In this case both components of friction with air are cumulated.

Following Burg [17] the total friction torque of the flywheel with air is the sum of the values (3) and (11) obtained above:

$$M_{fair} = M_{fdisk} + M_{frim} \quad (14)$$

Another estimation of the air friction torque gives [15] (that cites [16]) cumulating into a unique expression both components (6) and (13):

$$M_{f,air} = 0.0298 \cdot v^{0.2} \cdot \rho \cdot \left(\frac{d}{2}\right)^{3.9} \cdot \omega^{1.8} \cdot \left[b \cdot d^{-0.3} + 1.22147 \cdot \left(\frac{d}{2}\right)^{0.7} \right] \quad (15)$$

The total analytical friction torque is presented in Figure 5 . We can remark that the values obtained in references [15] and [16] are higher than those obtained in references [17] and [18].

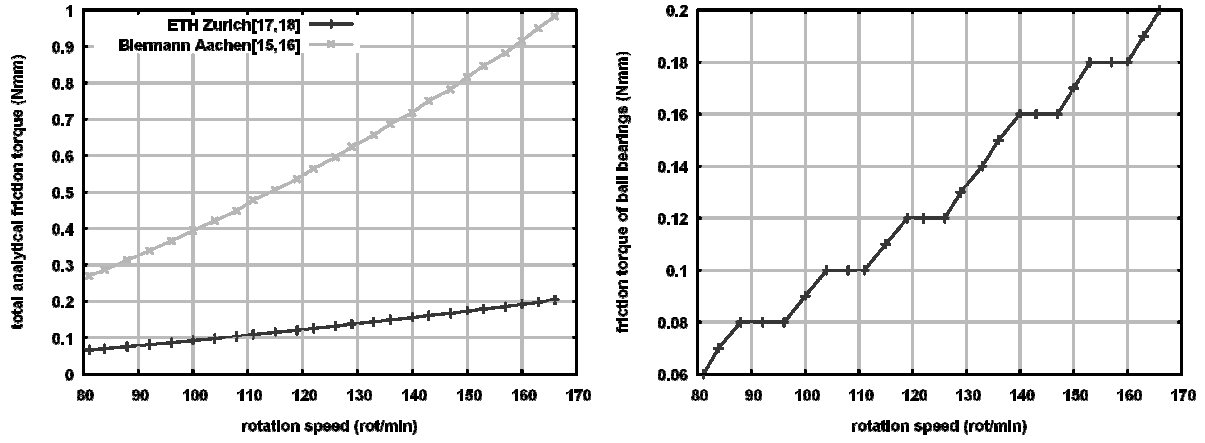


Figure 5 Total analytical friction torque and friction torque of ball bearings

4.1.4 Numerical model

A numerical model was realized using the Fluent CFD software. A turbulent k-ε model was used.

4.1.5 Friction torque of the ball bearings

The friction torque of the deep groove ball bearings was calculated using the SKF model for calculation of the frictional moment according to equation:

$$M_{fbb} = M_{rr} + M_{sl} + M_{seal} + M_{drag} \quad (5)$$

5. Results

The obtained experimental results for the variation of the rotational speed of the flywheel with time are presented in Figure 6. The temperature of the measurements was around 28 °C.

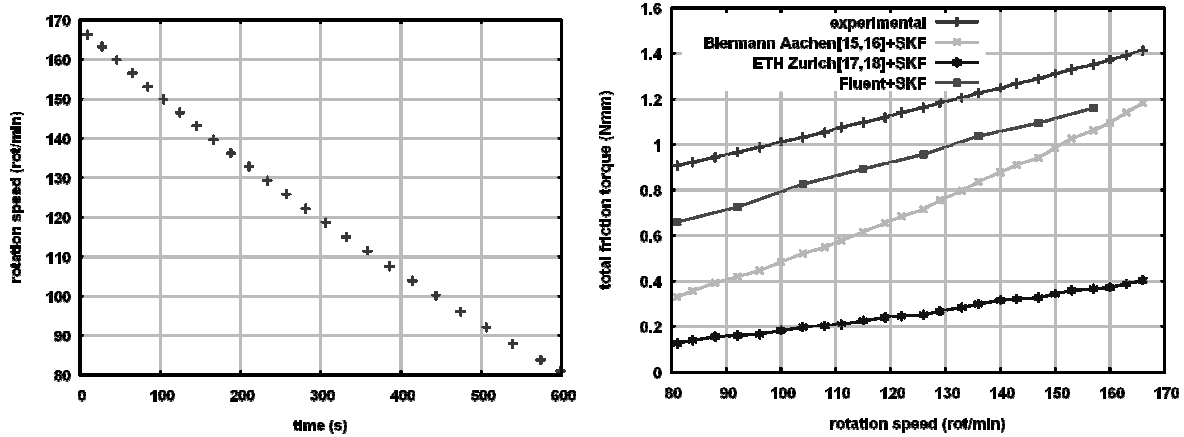


Figure 6 Variation of the rotation speed with time and of the friction torque with rotation speed

From these values we can compute the values of the friction torque function of time using the SKF the following formula:

$$M_{faiexp} = I_{flywheel} \frac{d\omega}{dt} \quad (6)$$

where the angular acceleration ($d\omega/dt$) is estimated using the fitted polynomial approximation of angular velocity:

$$\omega(t) = 17.5998 - 0.0190276 \cdot t + 7.56559 \cdot 10^{-6} \cdot t^2 - 2.01647 \cdot 10^{-9} \cdot t^3 \quad (7)$$

The theoretical and experimental values are presented in Figure 6. The analytical model which is closer to the experimental data is presented in references [15] and [16]. The obtained values using the other analytical models give smaller friction torque than those obtained in the experiments.

If the same flywheel would rotate at 20000 rot/min the flywheel would store 85% of the kinetic energy of a 2000kg vehicle at a speed of 50km/h. According to the model presented in [15] and [16] the flywheel would lose 11kW due to friction with air, which is considered to be high. If we replace in the same model the air with helium, the friction losses are of 2.2kW, which are considerably lower.

6. Conclusions

A good correlation can be observed between the experimental and numerical values obtained with the Fluent CFD software. The analytical models do not always give the same results. The analytical model which is closer to the

experimental data is presented in references [15] and [16]. The obtained values using the other analytical models give smaller friction torque than those obtained in the experiments. If the flywheel runs in a helium atmosphere, the friction torque is considerably lower compared to air.

References

- [1] <http://www.fbw.ch/galerie/gyrobus/gyrohoffnung.HTM>
- [2] Genta G.: Kinetic Energy Storage: Theory and Practice of Advanced Flywheel Systems. Butterworth-Heinemann Ltd, 1985
- [3] Laurian T., Marian V.G., Prisecaru T.: Experimental Analysis of a Kinetic Energy Recovery System Intended for Small and Medium Passenger Cars, in: Dobre, G. (Ed.), Power Transmissions, Mechanisms and Machine Science. Springer Netherlands, 2013, 347–355.
- [4] Dems K., Turant J.: Two approaches to the optimal design of composite flywheels. *Engineering Optimization* 41, 2009, 351–363
- [5] Arvin A., Bakis C.: Optimal design of press-fitted filament wound composite flywheel rotors. *Composite Structures* 72, 2006, 47–57
- [6] Portnov G., Uthe A.-N., Cruz I., Fiffe R.P., Arias F.: Design of Steel-Composite Multirim Cylindrical Flywheels Manufactured by Winding with High Tensioning and in situ Curing. 1. Basic Relations. *Mechanics of Composite Materials* 41, 2005, 139–152
- [7] Bai Y., Gao Q., Li H., Wu Y., Xuan M.: Design of composite flywheel rotor. *Frontiers of Mechanical Engineering in China* 3, 2008, 288–292
- [8] Krack M., Secanell M., Mertiny P.: Cost optimization of hybrid composite flywheel rotors for energy storage. *Structural and Multidisciplinary Optimization* 41, 2010, 779–795
- [9] Tzeng J., Emerson R., Moy P.: Composite flywheels for energy storage. *Composites Science and Technology* 66, 2520–2527, 2006
- [10] Filatov A.V., Maslen E.H.: Passive magnetic bearing for flywheel energy storage systems. *Magnetics, IEEE Transactions on* 37, 2002, 3913–3924.
- [11] Murakami K., Komori M., Mitsuda H., Inoue A.: Design of an energy storage flywheel system using permanent magnet bearing (PMB) and superconducting magnetic bearing (SMB). *Cryogenics* 47, 272–277.
- [12] Dai, 2001: On the vibration of rotor-bearing system with squeeze film damper in an energy storage flywheel. *International Journal of Mechanical Sciences* 43, 2007, 2525–2540.
- [13] Beitz W., Grote K.-H., Dubbel H.: *Dubbel - Taschenbuch für den Maschinenbau*, Auflage: 20., neubearb. u. erw. Aufl. ed. Springer, Berlin u.a, 2001
- [14] Childs P.: *Rotating Flow*, 1 edition. ed. Butterworth-Heinemann, Amsterdam; Boston, 2010
- [15] Raabe N.: Anlassen großer Asynchronmotoren in Schiffsbordnetzen, Dissertation, T. U. Hamburg-Harburg
- [16] Biermann, J. W. , 1981, Untersuchungen zum Einsatz von Schwungradenergiespeichern als Antriebselemente für Kraftfahrzeuge, Dissertation, RWTH-Aachen, 2010
- [17] Burg von P.: Schnelldrehendes Schwungrad aus faserverstärktem Kunststoff, Dissertation ETH Zürich).
- [18] Schlichting H.: *Grenzschicht-Theorie*, Braun, Karlsruhe , 1982
- [19] Neue Hütte. *Die Grundlagen der Ingenieurwissenschaften*, 29. Auflage, Springer Verlag, Berlin, Heidelberg, 1989